

# Analysis on the crossing obstacle of wheel-track hybrid mobile robot<sup>①</sup>

Shuai Liguó (帅立国)<sup>②\*</sup>, Fei Yanqiong<sup>\*\*</sup>, Zheng Liyuan<sup>\*</sup>, Gong Pengwei<sup>\*\*</sup>

(\* Henan Institute of Science and Technology, Xinxiang 453003, P. R. China)

(\*\* Research Institute of Robotics, Shanghai Jiaotong University, Shanghai, 200240, P. R. China)

## Abstract

A novel wheel-track hybrid mobile robot with many movement patterns is designed. According to different environments, it can switch between the pure wheel pattern and the pure track one. According to a homogeneous coordinate transformation matrix, gravity stability and its obstacle performance are analyzed. Its gravity equation and climbing obstacle conditions are established. Experimental results show that this hybrid mobile robot could fully possess the advantages of both the wheel and the track mechanisms and achieve a good obstacle climbing capability.

**Key words:** wheel-track hybrid robot, moving mechanism, obstacle performance

## 0 Introduction

Mobile robots are useful in many applications of dangerous environments, such as reconnaissance, patrol, vigilance and mine sweeping. There are mostly three kinds of moving mechanisms, like wheel-type structures, track-type structures, and leg-type structures. The wheel-type robot has a brief mechanism, low energy consume, agility movement, and a high migration velocity. But it also has some disadvantages, such as easily skidding in wet slippery soft road surface and weak adaptation in crossing obstacle<sup>[1]</sup>. The typical wheel-type robots are Nomad polar region exploration vehicle<sup>[2]</sup> and Shrimp robot<sup>[3]</sup>. Track-type robot has a big support area, good traction adhesion performance, and high adaptation in crossing obstacle. But its energy consumption is high and velocity is slow. There are some typical track-type robots, like Famous handcart Wheelbarrow EOD robot<sup>[4]</sup>, VIPER<sup>[5]</sup>, modularization EOD robot ASENDRO<sup>[6]</sup> and so on. The leg-type robot can satisfy some specific performances and has good adaptation in complex terrain, but its structure is too intricacy. DynaRoACH six foot robot<sup>[7]</sup> and roundness radial symmetry six foot robot<sup>[8]</sup> are the typical leg-type robots.

Although mobile robots have good advantages in complicated and changeable environment, a lot of problems still exist. Firstly the robots need to improve their stability and ability to adapt different environments. Secondly, the robots need to increase their

elasticity due to complicated constructions and big mass. Lastly, because of the existence of large friction resistance between the robot and the road surface, it is important to increase the efficiency<sup>[9]</sup>.

A novel wheel-track hybrid mobile robot is designed. Both the pure wheel pattern and the pure track pattern can be achieved in different conditions. The robot works with a pure wheel pattern when it moves in far distance on the flatness road. On the other hand, the robot works with the pure track pattern when it moves on an uneven road at outdoors.

## 1 Construction design of wheel-track hybrid mobile robots

### 1.1 Overall structure

With the symmetry construction, the mobile robot can move freely in narrow channel, without changing the direction or adjusting the body, which improves the operational efficiency. At the same time, it also increases the interchangeability of parts.

In Fig. 1, the mobile robot has a couple of differential wheels in the middle of body and a couple of guide wheels which are placed at the front and the back respectively. The robot is driven forward by differential wheels when it works with the pure wheel pattern. The track mechanism can not only drive track to rotate, but also swing around the axis of the driving wheel. The central body of the robot is between the track arms, which is the skeleton of mobile robot and mainly for installing embedded control systems, batteries, sensors

① Supported by the National Natural Science Foundation of China (No. 61175069, 51075272, 51475300).

② To whom correspondence should be addressed. E-mail: liguo.shuai@126.com

Received on Jan. 14, 2015

and some other necessary devices.

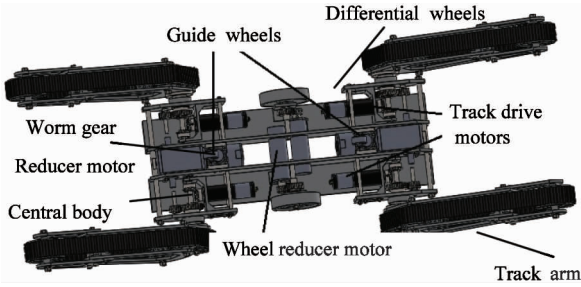


Fig. 1 The overall structure of the robot

The robot can switch between the track-type and the wheel-type by swinging track arms to achieve the pure track pattern by swinging track arms down and achieve the pure wheel pattern by swinging track arms up.

1.2 Power transmission system

There are eight degrees of freedom in the power-driven system of the robot, as shown in Fig. 2. The wheel part has 2 degrees of freedom. It can realize the high-speed motion, which is driven by a couple of DC motors through the straight teeth reduction gear. The rotation part of four track arms has 4 degrees of freedom, considering great resistance in the movement on poor road conditions. And the swinging part of track arms has 2 degrees of freedom. It is driven by a couple of DC motors through the worm gear reducer. In Fig. 1 and Fig. 2, the track arms at the same side of the robot body are driven by the same motor and they can swing 360°.

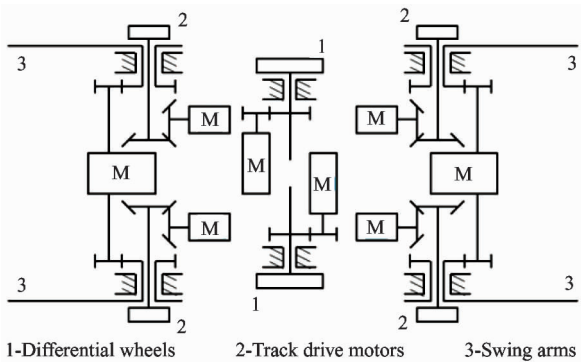


Fig. 2 Power transmission system of mobile robot

1.3 Driving device of track arms

Track arms mechanism can drive the tracks to rotate and swing, and both of these two different motions are achieved by rotating around the axis of the drive wheel. The track arms are driven by the reduction motor as shown in Fig. 3. The rotary motion of the track is

achieved by connecting the inner axis and the driving wheel together with a key, and the inner axis is powered by a couple of bevel gears. The small axis and the worm-gear motor are connected by a rigid coupling, which can keep the track arms driven by the same motor in accordance with each other. The power on the outside axis is transferred from the small axis by a pair of straight teeth reduction gear. On one hand, the reduction gear can take two central drive shafts of the motor apart, which is good for the transmission of different torques. On the other hand, it can increase the driving torque of the track arms.

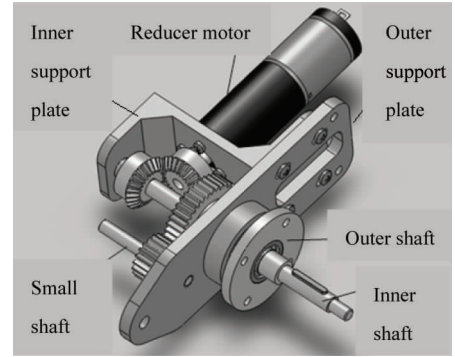


Fig. 3 Driving device of track arms

2 The motion analysis of crossing obstacle

2.1 The typical process of crossing obstacles

The track arms of the robot can swing 360°. The robot is abundant in state changes in crossing obstacle process. Fig. 4 shows the typical processes.

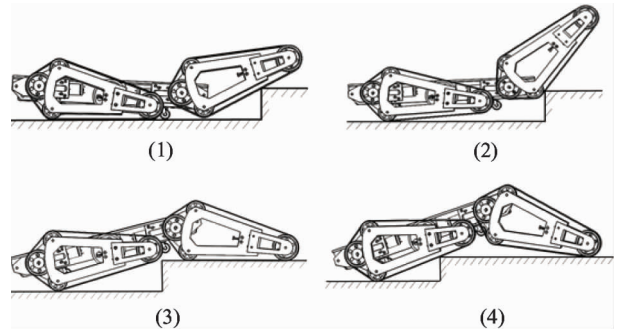


Fig. 4 The typical processes of crossing obstacle

2.2 Analysis on the gravity change of mobile robot

In Fig. 5, the Cartesian system  $o_1x_1y_1z_1$  and  $o_2x_2y_2z_2$  are established in the revolution axes of track arms, respectively. Coordinate  $o_1x_1y_1z_1$  is fixed in the central body, and coordinate  $o_2x_2y_2z_2$  is fixed to the right track arm.  $P_1(x_1, y_1, z_1)$  is the coordinate of gravity of the middle part,  $P_2(x_2, y_2, z_2)$  and  $P_3(x_3,$

$y_3, z_3$ ) are respectively the coordinates of gravity of the front track arms and the rear track arms,  $P^*(x^*, y^*, z^*)$  is the coordinate of gravity of the robot.  $\theta_1$  and  $\theta_2$  are the rotary angles for the track arms relative to the middle part of the body.  $l$  is the distance between the shaft and the gravity of the track arm.  $L$  is the distance between the rotary axis of two track arms. The coordinate of gravity  $P^*$  in coordinate  $o_1x_1y_1z_1$  is

$$\begin{aligned} \begin{pmatrix} x^* \\ y^* \\ z^* \\ 1 \end{pmatrix} &= \frac{1}{M} \cdot \left[ \begin{pmatrix} x_1 \\ y_1 \\ z_1 \\ 1 \end{pmatrix} \cdot m_1 + \begin{pmatrix} x_2 \\ y_2 \\ z_2 \\ 1 \end{pmatrix} \cdot m_2 + \begin{pmatrix} x_3 \\ y_3 \\ z_3 \\ 1 \end{pmatrix} \cdot m_2 \right] \\ &= \frac{1}{M} \cdot \left[ \begin{pmatrix} x_1 \\ y_1 \\ 0 \\ 1 \end{pmatrix} \cdot m_1 + \begin{pmatrix} l \cdot \cos\theta_1 \\ l \cdot \sin\theta_1 \\ 0 \\ 1 \end{pmatrix} \cdot m_2 \right] \\ &\quad + {}_1^2Trans \cdot {}_2^1Rot \cdot \begin{pmatrix} l \\ 0 \\ 0 \\ 1 \end{pmatrix} \cdot m_2 \end{aligned} \quad (1)$$

$$M = (m_2 + 2 \cdot m_1) \quad (2)$$

where,  $m_1$ ,  $m_2$ , and  $M$  are the mass of the central body, the track arms, and the whole robot respectively.  ${}_1^2Trans$  and  ${}_2^1Rot$  are the homogeneous coordinate translation matrix and the rotation matrix of the coordinate system  $o_2x_2y_2z_2$  relative to the coordinate system  $o_1x_1y_1z_1$ .

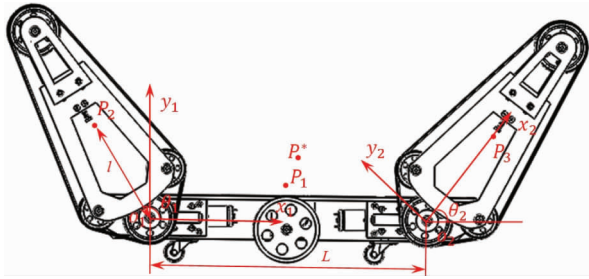


Fig. 5 Gravity of the robot

Assuming that two swing arms at the right side are fixed, the relation between  $x^*$  and  $y^*$  is obtained

$$\begin{aligned} \left[ x^* - \frac{m_1 \cdot x_1 + (l \cdot \cos\theta_2 + L) \cdot m_2}{M} \right]^2 \\ + \left[ y^* - \frac{m_1 \cdot y_1 + m_2 \cdot l \cdot \sin\theta_2}{M} \right]^2 = \left[ \frac{m_2 \cdot l}{M} \right]^2 \end{aligned} \quad (3)$$

According to Eq. (3), the gravity ( $x^* y^*$ ) of the robot is located within the circle of radius  $R \leq m_2 \cdot l/M$ . So, when the length of the track arms and the load capacity meet the conditions, the mass of the track arms  $m_2$  should be light and the position of gravity of track arms should be close to the rotation axis in or-

der to increase the movement stability.

## 2.3 Conditions of climbing over obstacle

### 2.3.1 Climbing over obstacle in translational motion

The ability of robot's crossing obstacle is defined as vertical that it can just get over. The robot can climb over the obstacle when the vertical line of the gravity overpasses the vertical wall edge in furthest possible erection process<sup>[10]</sup>.

Coordinate system  $o_0x_0y_0z_0$  is the base coordinate system fixed on the ground, supposing the coordinate  $P^*$  is  $(x, y, z)$  in the base coordinate system  $o_0x_0y_0z_0$ . In Fig. 6, the distance between the wheel center  $o_1$  of driving wheel of the track arms and the wheel center  $o_3$  of the small pulley is  $R$ . The radius of the small pulley is  $r$ . The rotary angle of the coordinate system  $o_1x_1y_1z_1$  relative to the base coordinate system is  $\theta$ . The following equation could be established to cross obstacle.

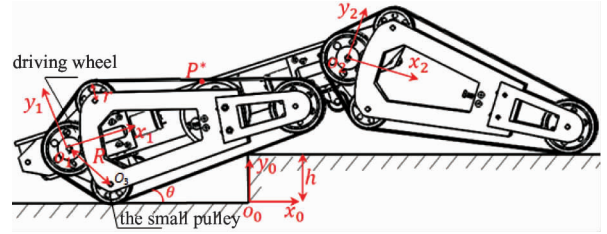


Fig. 6 The figure of robot's crossing obstacle

$$\begin{aligned} \begin{pmatrix} x \\ y \\ z \\ 1 \end{pmatrix} &= {}_1^0Trans \cdot {}_1^0Rot \cdot \begin{pmatrix} x^* \\ y^* \\ z^* \\ 1 \end{pmatrix} = \\ &\begin{pmatrix} 1 & 0 & 0 & -\frac{h}{\tan\theta} - r \cdot \tan\frac{\theta}{2} - R \cdot \cos(60^\circ - \theta) \\ 0 & 1 & 0 & r + R \cdot \sin(60^\circ - \theta) \\ 0 & 0 & 1 & 0 \\ 0 & 0 & 0 & 1 \end{pmatrix} \\ &\cdot Rot(z_0, \theta) \cdot \begin{pmatrix} x^* \\ y^* \\ z^* \\ 1 \end{pmatrix} = \\ &\begin{pmatrix} x^* \cdot \cos\theta - y^* \cdot \sin\theta - \frac{h}{\tan\theta} - r \cdot \tan\frac{\theta}{2} - R \cdot \cos(60^\circ - \theta) \\ x^* \cdot \sin\theta + y^* \cdot \cos\theta + r + R \cdot \sin(60^\circ - \theta) \\ 0 \\ 1 \end{pmatrix} \end{aligned} \quad (4)$$

where,  $h$  is the height of the step,  ${}_1^0Trans$  is the homogeneous coordinate translation matrix on the coordinate system  $o_1x_1y_1z_1$  relative to the base coordinate system  $o_0x_0y_0z_0$ , and  ${}_1^0Rot$  is the rotation matrix.

when  $x = 0$ ,

$$h = x^* \cdot \sin\theta - y^* \cdot \sin\theta \cdot \tan\theta - r \cdot \tan\theta \cdot \tan(\theta/2) - R \cdot \cos(60^\circ - \theta) \cdot \tan\theta \quad (5)$$

According to Eqs(4) and (5), when the geometry parameters of the robot are fixed, the coordinates of center point  $P^*$  are the functions of  $h$  and  $\theta$ . The gravity  $(x, y, z)$  of the robot will have different tracks in the base coordinate system  $o_0x_0y_0z_0$  with different height  $h$ . The parameters are given in Table 1.

Table 1

Mass	Length	Coordinate	Radius	Angle
$m_1 = 12\text{kg}$	$L = 380\text{mm}$	$x_1 = 190\text{mm}$	$R = 70\text{mm}$	$\theta_1 = -10^\circ$
$m_2 = 3\text{kg}$	$l = 95\text{mm}$	$y_1 = 5\text{mm}$	$r = 27.5\text{mm}$	$\theta_2 = -35^\circ$

The maximum rotary angle  $\theta$  is  $60^\circ$  because of the robot's structure. When the robot crosses obstacles, the gravity  $(x, y, z)$  in the base coordinate system is shown in Fig. 7.

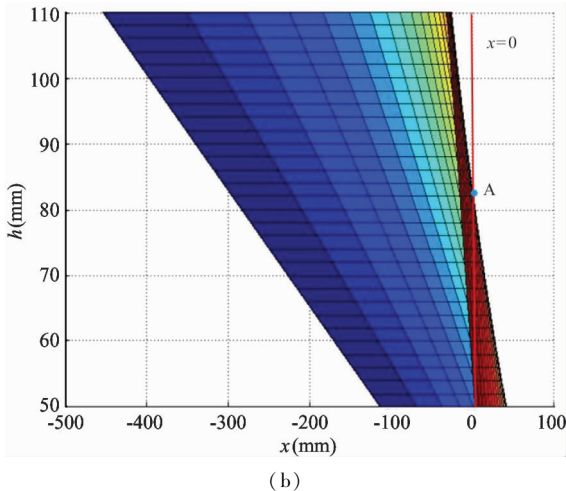
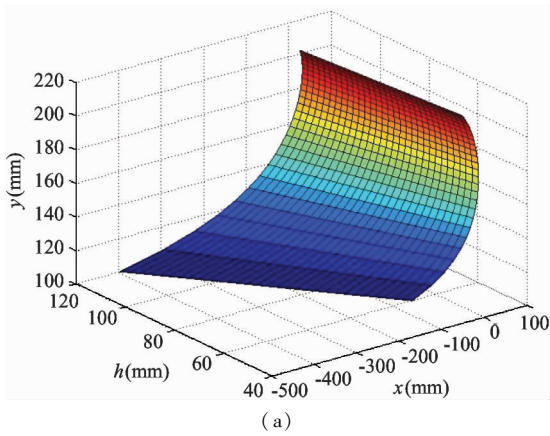


Fig. 7 The gravity trajectory of the robot when crossing over obstacle with different heights

If the gravity trajectory of the robot can cross over the plane  $x = 0$ , the robot will have the capacity of

crossing the obstacle. In Fig. 7, the gravity trajectory of the robot can overpass the plane  $x = 0$  only when the height of the obstacle is less than point A. The coordinate of point A on the  $h$  axis is 81.947. So the height of the obstacle that this mobile robot can climb over is 81.947mm.

### 2.3.2 Climbing over obstacle with swing arms

When it runs into high obstacles, the wheel-track hybrid mobile robot climbs over the obstacle mostly depending on the swinging action of track arms. The critical position of this way is shown in Fig. 8.

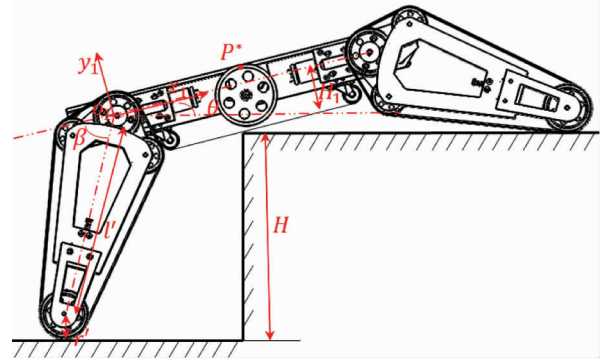


Fig. 8 The critical position of mobile robot climbing over obstacle with swing arms

In Fig. 8, where,  $\theta$  is the angle between the horizontal axis in the coordinate system  $o_1x_1y_1z_1$  and the horizontal direction.  $H$  is the height of obstacle,  $H_1$  is the vertical distance between the swinging arm axis and the bottom of the wheel.  $l'$  is the distance between the swing arm axis and the big driven pulley,  $r'$  is the radius of the big driven pulley,  $\beta$  is the angle between the center line of the swing arm and the axis  $x_1$ . According to the geometrical relationship in Fig. 8, the following is got

$$H + \frac{H_1 + y^*}{\cos\theta} = r' + l' \cdot \cos(90^\circ - \theta - \beta) + x^* \cdot \sin\theta + y^* \cdot \cos\theta \quad (6)$$

In the equation:  $x^*, y^*$  are coordinates of the gravity in coordinate system  $o_1x_1y_1z_1$ , and Eq. (6) can be arranged,

$$H = r' + l' \cdot \cos(90^\circ - \theta - \beta) + x^* \cdot \sin\theta + y^* \cdot \cos\theta - \frac{H_1 + y^*}{\cos\theta} \quad (7)$$

It is obvious that rotary angle  $\theta$  of the central body and rotary angle  $\beta$  of the track arms have great influence on the height of the obstacle. Donote  $r' = 30\text{mm}$ ,  $l' = 300\text{mm}$ ,  $H_1 = 60\text{mm}$ , we can obtain the relations between height  $H$  and rotary angle  $\theta, \beta$ , in Fig. 9.

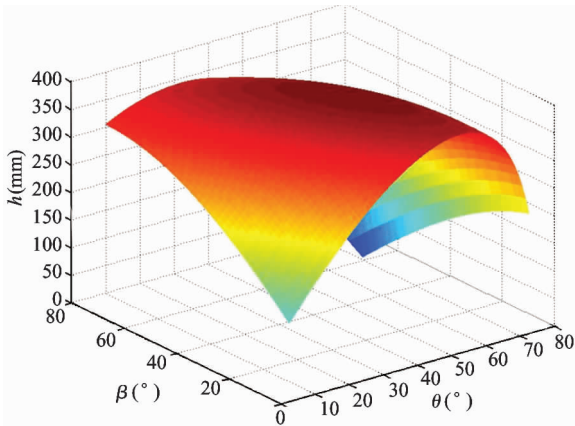


**Fig. 9** Relations between the obstacle height and the rotary angles of the body and the swing arms

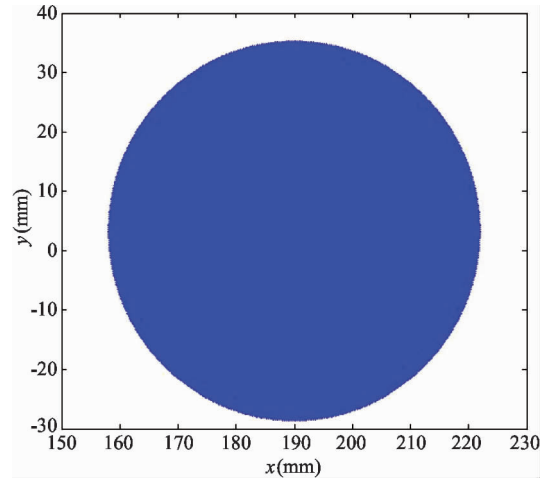


**Fig. 12** The trajectory of the gravity on the mobile robot

### 3 Experiments

Fig. 10 illustrates the experiment of the wheel-type movement in room, and Fig. 11 shows the experiment of climbing over the obstacle about 80mm. Both of them can be finished successfully. When these four track arms swing  $360^\circ$  around the rotary axis, the trajectory of point  $P^*$  is shown in Fig. 12.

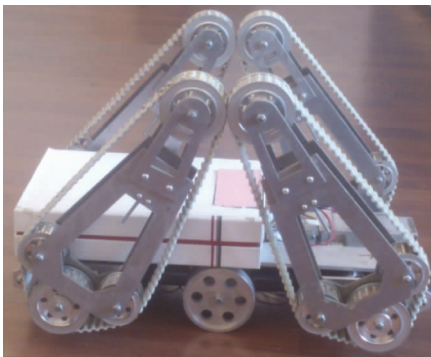


**Fig. 10** Wheel-type movement of the robot

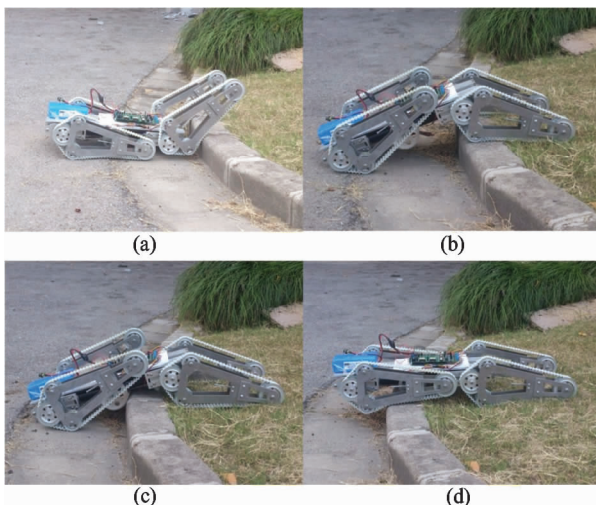


**Fig. 11** Climbing over the obstacle

### 4 Conclusions

A new wheel-track hybrid mobile robot is developed. It performs well both in indoor flat environment and outdoors complicated environment. The robot has a variety of movement modes. It can switch between the pure wheel pattern and the pure track pattern. The robot can achieve the pure track pattern by swinging track arms down and achieve the pure wheel pattern by swinging track arms up. The conditions of climbing over obstacle based on the homogeneous coordinate transformation matrix are analyzed. The relationship between the robot's gravity and the obstacle's height as well as rotary angles of the track is established. The experiments of the wheel-type movement in door and climbing over the obstacle outdoors are shown. Compared with the similar mobile robot, it has the advantages of smaller volume, compacter structure, higher energy efficiency and so on.

### References

- [ 1 ] Zhu L L, Chen J. A review of wheeled mobile robots research. *Machine Tool & Hydraulics*, 2009, 37(8) : 242-247
- [ 2 ] Chopra A, Obsniuk M, Jenkin M R. The nomad 200 and the nomad super scout; reverse engineered and resurrected. In: *Proceedings of the 3rd Canadian Conference on Computer and Robot Vision*, Quebec, Canada, 2006. 55-55
- [ 3 ] Dian S, Liu T, Liang Y, et al. A novel shrimp rover-based mobile robot for monitoring tunnel power cables. In: *Proceedings of the 2011 International Conference on Mechatronics and Automation (ICMA)*, Beijing, China, 2011. 887-892
- [ 4 ] Szynekarczyk P, Czupryniak R, Trojnecki M, et al. Current state and development tendency in mobile robots for special applications. In: *Proceedings of the International*

- Conference WEISIC, Bucharest, Romania, 2008, 8: 30-41
- [ 5 ] Vu Q H, Kim B S, Song J B. Autonomous stair climbing algorithm for a small four-tracked robot. In: Proceedings of the International Conference on Control, Automation and Systems, Seoul, Korea, 2008. 2356-2360
- [ 6 ] Edlinger R, Pözlleithner A, Zauner M. Mechanical Design and System Architecture of a Tracked Vehicle Robot for Urban Search and Rescue Operations. Research and Education in Robotics-EUROBOT 2010. Springer Berlin Heidelberg, 2011. 46-56
- [ 7 ] Hoover A M, Burden S, Fu X Y, et al. Bio-inspired design and dynamic maneuverability of a minimally actuated six-legged robot. In: Proceedings of the 3rd IEEE RAS and EMBS International Conference on Biomedical Robotics and Biomechatronics (BioRob), Tokyo, Japan, 2010. 869-876
- [ 8 ] Wang Z, Ding X, Rovetta A, et al. Mobility analysis of the typical gait of a radial symmetrical six-legged robot. *Mechatronics*, 2011, 21(7): 1133-1146
- [ 9 ] Si Y Y, Zhao X H, Shi C H, et al. Walking mechanism design and kinematic analysis of wheel-tracked composite robot. *Machinery Design & Manufacture*, 2013, (7). doi: 103969/j. issn. 1001-3997. 2013. 07. 061 (In Chinese)
- [10] Merhop W, Hackbarth E M. Tracked vehicle mechanics. Han xuemei. Beijing: National Defence Industry Press, 1989

**Shuai Ligu**, born in 1968. He received his Ph. D degree and M. S degree in School of Instrument Science & Engineering of Southeast University in 2001 and 1998. He also received his B. S. degree from Xi'an JiaoTong University in 1991. His research interests include the intelligent robots, the technology of tactile display and the virtual reality technology.